

## Supporting Information

### **A highly robust metal-organic framework based on an aromatic 12-carboxyl ligand with highly selective adsorption of CO<sub>2</sub> over CH<sub>4</sub>**

Hongming He,<sup>a</sup> Yang Song,<sup>a</sup> Chuanqi Zhang,<sup>a</sup> Fuxing Sun,<sup>a\*</sup> Rongrong Yuan,<sup>a</sup> Zheng Bian,<sup>b\*</sup> Lianxun Gao<sup>b</sup> and Guangshan Zhu<sup>a</sup>

**S1.** Materials and measurements

**S2.** Synthesis

**S3.** X-ray structure determination and structure refinement

**Fig. S1** FT-IR spectra of **H<sub>12</sub>TDDPB** and **JUC-132**

**Fig. S2** The asymmetric unit of **JUC-132**

**Fig. S3** Two adjacent ligands are connected by Cd(II) ions

**Fig. S4** The cage is surrounded by two adjacent ligands and connected by six Cd(II) ions

**Fig. S5** Excitation and emission spectra of **JUC-132**

**Fig. S6** PXRD patterns of simulated, activated and as-synthesized samples

**Fig. S7** PXRD patterns of **JUC-132** in different environments

**Fig. S8** TGA plots desolvated (red) and solvated (black) form of **JUC-132** in air

**Fig. S9** FT-IR spectra of activated samples

**Fig. S10** The N<sub>2</sub> sorption isotherms of **JUC-132** at 77 K

**Fig. S11** Pore size distribution calculated by Horvath-Kawazoe (HK) model

**Fig. S12** Calculated isosteric heats of adsorption for CO<sub>2</sub> uptake

**Fig. S13** Calculated isosteric heats of adsorption for CH<sub>4</sub> uptake

**Fig. S14** The SEM pictures of solvated bulk crystals

**Fig. S15** The photographs of solvated bulk crystals

**S4.** IAST calculations

**Table S1.** Summary of the parameters calculated by IAST theory at 273 K and 298 K

**Table S2.** Crystal data and structure refinement for **JUC-132**

**Table S3.** Selected bond lengths (Å) and angles (deg) for **JUC-132**

**S5.** References

## S1. Materials and measurements

All the chemical reagents were obtained from commercial sources and used without further purification. Elemental analyses (C, H and N) were acquired on a Perkin-Elmer 240 analyzer. Powder X-ray-diffraction (PXRD) measurements were performed on a Scintag X1 diffractometer with Cu-K $\alpha$  ( $\lambda = 1.5418 \text{ \AA}$ ) at 50 kV, 200 mA with a  $2\theta$  range of 4-40° at room temperature. Thermogravimetric analyses (TGA) were performed with a Perkin-Elmer TGA thermogravimetric analyzer in the range of 30-800 °C under air flow at a heating rate of 10 °C/min for all measurements. Fourier-transform infrared spectra (FT-IR) were obtained in the 4000-400  $\text{cm}^{-1}$  range using a Nicolet Impact 410 FT-IR spectrometer (KBr pellets). Gas sorption-desorption measurements were acquired on Autosorb-iQ2-MP-AG. All fluorescence measurements were recorded on a Fluoromax-4 Spectrofluorometer at room temperature. The morphologies and detailed structure of the samples were recorded using JEOL JSM-6700F field-emission scanning electron microscope (SEM).

## S2. Synthesis

Synthesis of  $[\text{Cd}_{15}(\text{TDDPB})_4(\text{H}_2\text{O})_6] \cdot 18[\text{H}_2\text{N}(\text{CH}_3)_2] \cdot 18\text{DMA}$  (**JUC-132**)

A mixture of  $\text{Cd}(\text{NO}_3)_2 \cdot 4\text{H}_2\text{O}$  (10 mg, 0.04 mmol), **H<sub>12</sub>TDDPB** (5 mg, 0.0039 mmol), DMAc (5 ml), H<sub>2</sub>O (0.3 ml) and 1.25 ml of an aqueous HNO<sub>3</sub> solution (2 M) was sealed into a 20 ml capped vessel and stirred for 15 minutes at room temperature. The mixture was heated at 100 °C for 2 weeks and then allowed to cool to room temperature to obtain the product as yellow crystals with the yield of 58 % (based on Cd). Element analysis (%) Calc. for  $\text{C}_{396}\text{H}_{438}\text{O}_{120}\text{N}_{36}\text{Cd}_{15}$ : C, 51.10; H, 4.71; N, 5.42; Found: C, 50.69; H, 4.67; N, 5.51. Selected FT-IR data (KBr pellet,  $\text{cm}^{-1}$ ): 3091 (br), 2532 (br), 1712 (s), 1596 (s), 1432 (s), 1218 (s), 862 (s), 757 (s), 659 (m), 524 (s). The organic ligand **H<sub>12</sub>TDDPB** was prepared according to literature procedures.<sup>[1]</sup>

## S3. X-ray structure determination and structure refinement

Crystallographic data collections for **JUC-132** were collected on Bruker SMART APEX II CCD based diffractometer equipped with graphite monochromatized Mo-K $\alpha$  radiation ( $\lambda = 0.71073 \text{ \AA}$ ) at 298K. Corrections for incident and diffracted beam absorption effects were applied to the data using the SADABS program.<sup>[2]</sup> The structures were solved by a combination of direct methods and refined by the full matrix least-squares against  $F^2$  values using the SHELXTL program.<sup>[3]</sup> All non-hydrogen atoms were located successfully from Fourier maps and were refined anisotropic thermal parameters. Crystallographic data for the structure are listed in Table S2 and the selected bond lengths and bond angles are reported in Table S3.

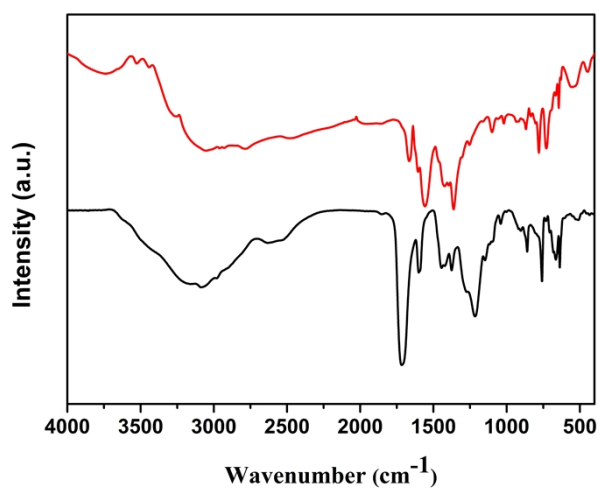


**Fig. S1** FT-IR spectra of  $H_{12}TDDPB$  (black) and activated  $JUC-132$  (red). The characteristic peak of carbonyl asymmetric stretching band (C=O) of  $-COOH$  at  $1712\text{ cm}^{-1}$  was only found in the black curve, implying that all carboxyl groups of ligand are deprotonated. The characteristic peak of C=O of DMAC molecules at  $1665\text{ cm}^{-1}$  was disappeared in the desolvated samples, implying that all guest DMAC molecules were removed completely.

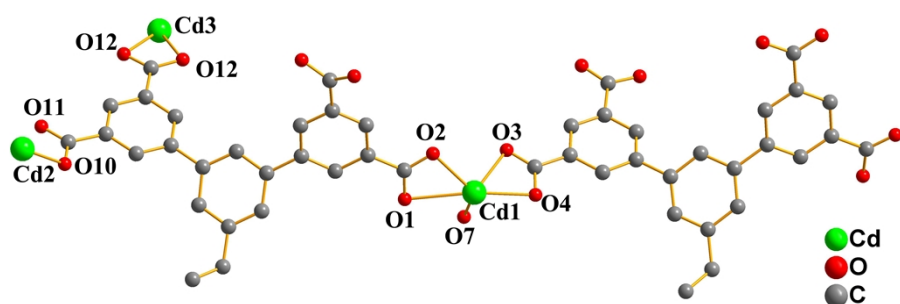


**Fig. S2** The asymmetric unit of  $JUC-132$ .

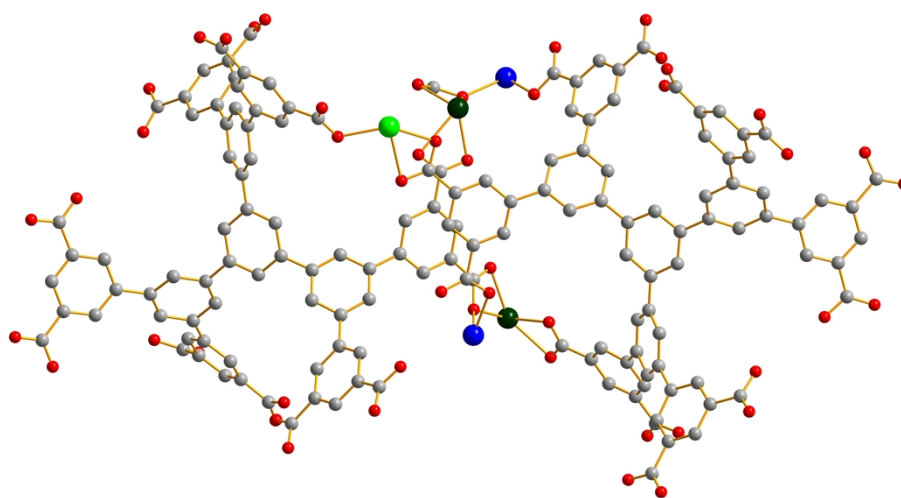


**Fig. S3** Two adjacent ligands are connected by Cd(II) ions.

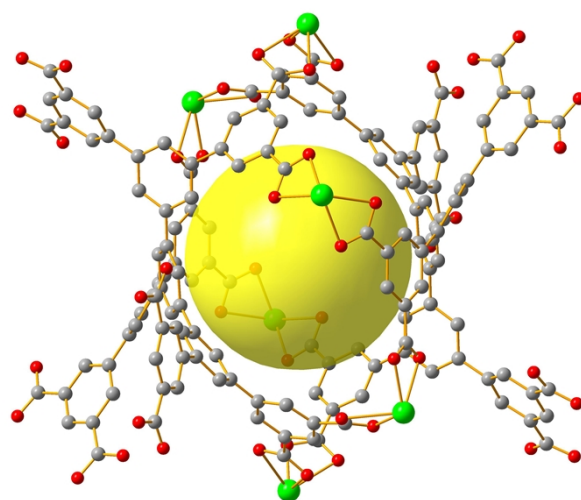


Fig. S4 The cage is surrounded by two adjacent ligands and connected by six Cd(II) ions.

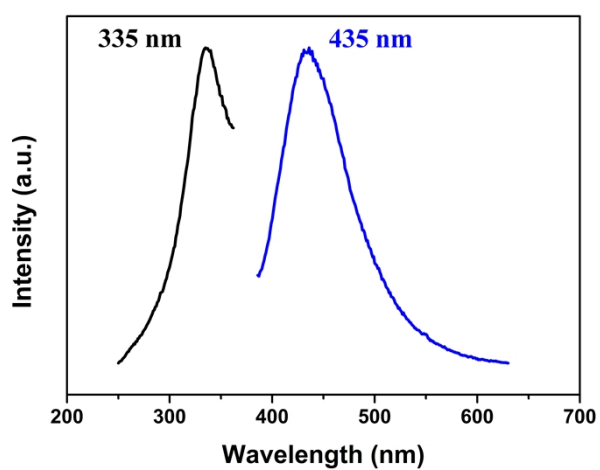


Fig. S5 Excitation (black) and emission (blue) spectra of JUC-132.

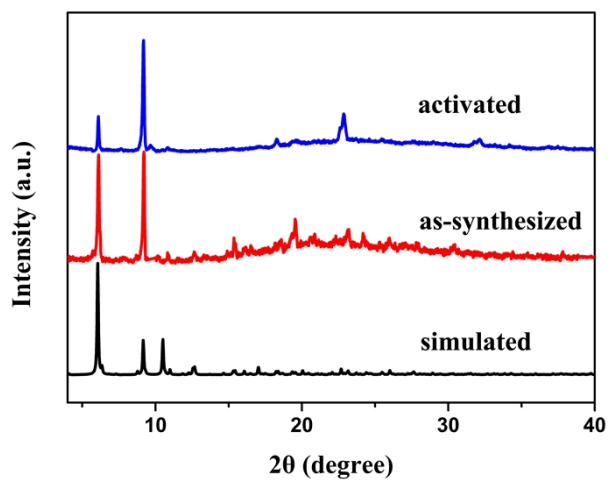


Fig. S6 PXRD patterns of simulated, as-synthesized and activated samples.

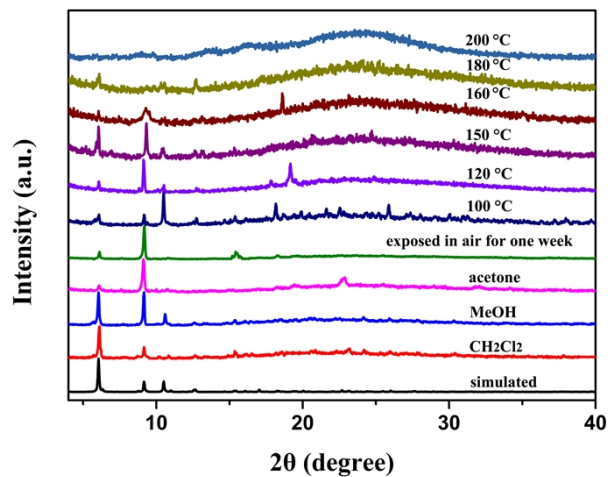


Fig. S7 PXR D patterns of JUC-132 in different environments.

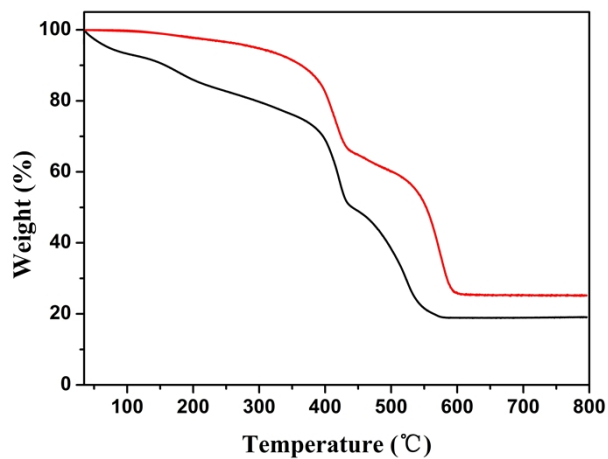
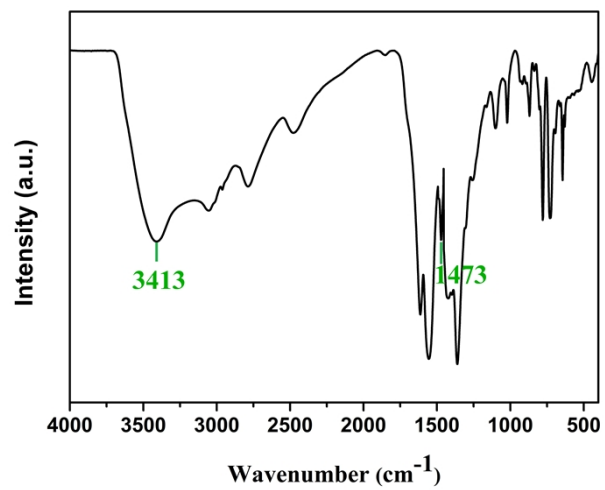
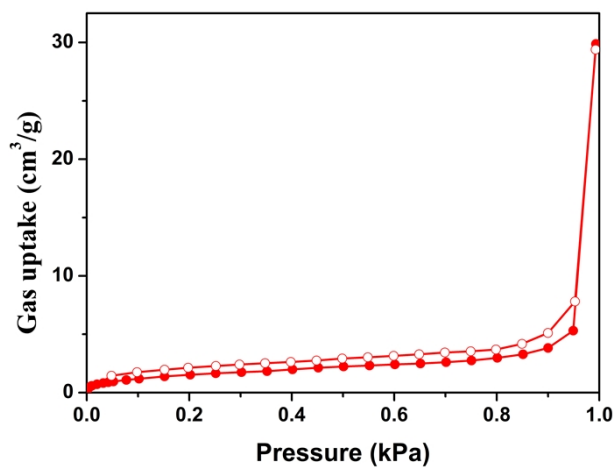


Fig. S8 TGA plots of desolvated (red) and solvated (black) form of JUC-132 in air.



**Fig. S9** FT-IR spectra of the activated sample. The peaks at 3413 and 1473  $\text{cm}^{-1}$  correspond to the stretching vibration of N-H and C-N bonds in  $\text{H}_2\text{N}(\text{CH}_3)_2$ , respectively.



**Fig. S10** The  $\text{N}_2$  sorption isotherms of JUC-132 at 77 K. Solid symbols, adsorption; open symbols, desorption.

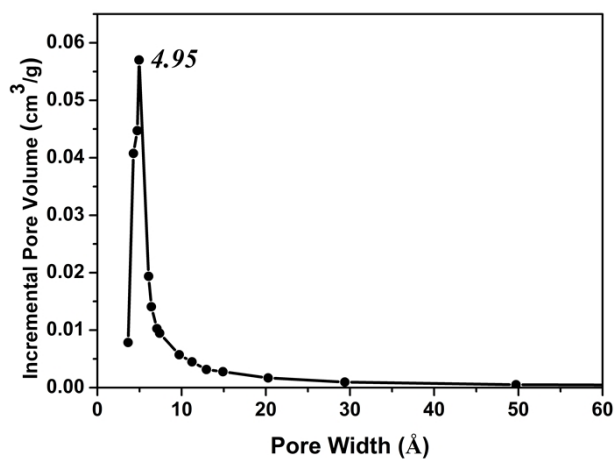


**Fig. S11** Pore size distribution calculated by Horvath-Kawazoe (HK) model.

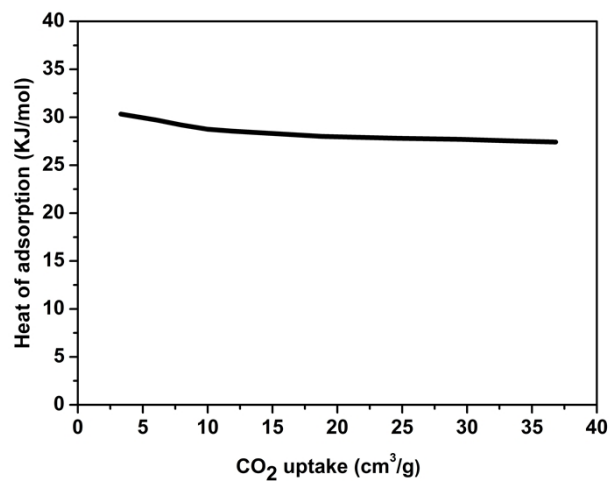


Fig. S12 Calculated isosteric heats of adsorption of CO<sub>2</sub> in JUC-132.

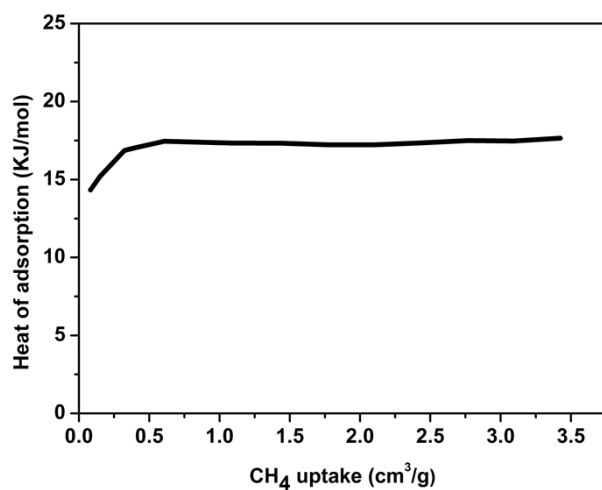


Fig. S13 Calculated isosteric heats of adsorption of CH<sub>4</sub> in JUC-132.

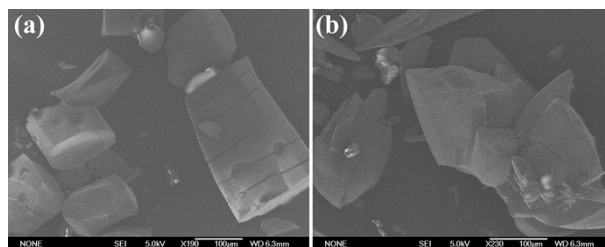
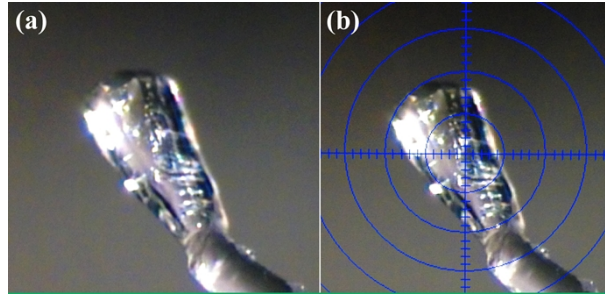


Fig. S14 The SEM pictures of solvated bulk crystals.



**Fig. S15** Images of solvated bulk **JUC-132** crystals (20  $\mu\text{m}$  for one scale) from single crystal X-ray different measurement.

#### S4. IAST Calculations

The adsorption isotherms for pure  $\text{CO}_2$  and  $\text{CH}_4$ , measured at 273 K and 298 K, were first converted to absolute loadings according to Peng-Robinson Equation. In order to perform the IAST calculation, the single-component gas absorption isotherms was fitted by the dual-site Langmuir-Freundlich (DSLFL) adsorption model, which was adopted to correlate the pure-component equilibrium data and further to evaluate the adsorption of binary gas mixtures. The DSLFL model is described as

$$N^0(f) = N_1 k_1 f / (1 + k_1 f) + N_2 k_2 f / (1 + k_2 f) \quad (1)$$

where  $f$  is the fugacity of bulk gas at equilibrium with adsorbed phase,  $N_i$  is the model parameter of the maximum adsorption amount at the site  $i$  ( $i = 1$  or  $2$ ) and  $k_i$  is the affinity constant.

Based on the above model parameters of pure gas adsorption, we used the IAST model, which was proposed by Myer and Prausnitz in 1965 to predict the multi-component adsorption.

**Table S1.** Summary of the parameters of the experimentally measured gas adsorption isotherms of **JUC-132** at 273 K and 298 K fitted with dual-site Langmuir-Freundlich adsorption model-based IAST theory.

<b>T</b>	273 K		298K	
	$\text{CO}_2$	$\text{CH}_4$	$\text{CO}_2$	$\text{CH}_4$
<b>bR<sup>2</sup></b>	0.99995	0.99999	0.99999	0.99992
<b>a<sub>1</sub></b>	0.92564	8	0.15404	1
<b>a<sub>2</sub></b>	3.2935	1	2.83168	2
<b>b<sub>1</sub></b>	0.10117	1.33748E-4	0.1292	9.13898E-5
<b>b<sub>2</sub></b>	0.01309	0.00214	0.01229	7.96278E-4
<b>c<sub>1</sub></b>	1	1	1	1
<b>c<sub>2</sub></b>	1	1	1	1

**Table S2.** Crystal data and structure refinement for **JUC-132**

Compound	<b>JUC-132</b>
Empirical formula	C <sub>132</sub> H <sub>146</sub> O <sub>40</sub> N <sub>12</sub> Cd <sub>5</sub>
Formula weight	3100.1
Temperature	293(2) K
Wavelength	0.71073 Å
Unit cell dimension	$a = 29.1653(9)$ Å, $b = 29.1653(9)$ Å, $c = 83.513(6)$ Å $\alpha = 90^\circ$ , $\beta = 90^\circ$ , $\gamma = 120^\circ$
Crystal System	Trigonal
Space group	<i>R</i> -3c
Volume	61520(5) Å <sup>3</sup>
Z	18
Calculated density	1.117 g / cm <sup>3</sup>
Mu	0.823 mm <sup>-1</sup>
F(000)	20304
Crystal size	0.45 mm × 0.40 mm × 0.30 mm
R(int)	0.0622
Nref	11840
Goodness-of-fit on F <sup>2</sup>	1.086
Final R indices [ $I > 2\sigma(I)$ ]	$R_1 = 0.0853$ , $wR_2 = 0.2596$
R indices (all data)	$R_1 = 0.1194$ , $wR_2 = 0.3105$

**Table S3.** Selected bond lengths (Å) and angles (deg) for **JUC-132**.

<b>JUC-32</b>			
Cd(1)-O(7)	2.262(8)	Cd(1)-O(2)	2.273(7)
Cd(1)-O(4)	2.301(7)	Cd(1)-O(6)#1	2.373(7)
Cd(1)-O(3)	2.421(8)	Cd(1)-O(5)#1	2.468(7)
Cd(1)-O(1)	2.562(8)	Cd(2)-O(17)#2	2.149(7)
Cd(2)-O(15)#3	2.153(9)	Cd(2)-O(12)	1 2.329(7)
Cd(2)-O(5)#4	2.377(7)	Cd(2)-O(13)	2.384(7)
Cd(3)-O(10)#4	2.229(8)	Cd(3)-O(10)	2.229(8)
Cd(3)-O(8)#5	2.289(7)	Cd(3)-O(8)#6	2.289(7)
Cd(3)-O(9)#5	2.528(8)	Cd(3)-O(9)#6	2.528(8)
O(5)-Cd(2)#4	2.377(7)	O(5)-Cd(1)#7	2.468(7)
O(6)-Cd(1)#7	2.373(7)	O(8)-Cd(3)#8	2.289(7)
O(9)-Cd(3)#8	2.528(8)	O(15)-Cd(2)#3	2.153(9)
O(17)-Cd(2)#9	2.149(7)		
O(7)-Cd(1)-O(2)	120.0(3)	O(7)-Cd(1)-O(4)	87.3(3)
O(2)-Cd(1)-O(4)	139.6(3)	O(7)-Cd(1)-O(6)#1	91.5(3)
O(2)-Cd(1)-O(6)#1	113.2(3)	O(4)-Cd(1)-O(6)#1	93.6(3)
O(7)-Cd(1)-O(3)	78.3(3)	O(2)-Cd(1)-O(3)	99.6(3)
O(4)-Cd(1)-O(3)	54.3(3)	O(6)#1-Cd(1)-O(3)	146.3(3)
O(7)-Cd(1)-O(5)#1	143.8(3)	O(2)-Cd(1)-O(5)#1	87.3(3)
O(4)-Cd(1)-O(5)#1	84.8(3)	O(6)#1-Cd(1)-O(5)#1	54.0(2)

O(3)-Cd(1)-O(5)#1	123.1(3)	O(7)-Cd(1)-O(1)	77.3(3)
O(2)-Cd(1)-O(1)	53.3(3)	O(4)-Cd(1)-O(1)	164.5(3)
O(6)#1-Cd(1)-O(1)	85.3(3)	O(3)-Cd(1)-O(1)	122.5(3)
O(5)#1-Cd(1)-O(1)	106.7(3)	O(17)#2-Cd(2)-O(15)#3	133.4(4)
O(17)#2-Cd(2)-O(12)	135.5(3)	O(15)#3-Cd(2)-O(12)	90.9(4)
O(17)#2-Cd(2)-O(5)#4	93.3(3)	O(15)#3-Cd(2)-O(5)#4	83.3(3)
O(12)-Cd(2)-O(5)#4	95.6(3)	O(17)#2-Cd(2)-O(13)	111.7(3)
O(15)#3-Cd(2)-O(13)	90.5(4)	O(12)-Cd(2)-O(13)	55.1(3)
O(5)#4-Cd(2)-O(13)	150.0(2)	O(17)#2-Cd(2)-O(14)#3	92.9(3)
O(15)#3-Cd(2)-O(14)#3	49.5(4)	O(12)-Cd(2)-O(14)#3	121.3(3)
O(5)#4-Cd(2)-O(14)#3	115.8(3)	O(13)-Cd(2)-O(14)#3	80.5(3)
O(10)#4-Cd(3)-O(10)	86.3(5)	O(10)#4-Cd(3)-O(8)#5	133.0(3)
O(10)-Cd(3)-O(8)#5	109.0(3)	O(10)#4-Cd(3)-O(8)#6	109.0(3)
O(10)-Cd(3)-O(8)#6	133.0(3)	O(8)#5-Cd(3)-O(8)#6	92.6(4)
O(10)#4-Cd(3)-O(9)#5	87.4(3)	O(10)-Cd(3)-O(9)#5	143.5(3)
O(8)#5-Cd(3)-O(9)#5	53.6(3)	O(8)#6-Cd(3)-O(9)#5	82.8(3)
O(10)#4-Cd(3)-O(9)#6	143.5(3)	O(10)-Cd(3)-O(9)#6	87.4(3)
O(8)#5-Cd(3)-O(9)#6	82.8(3)	O(8)#6-Cd(3)-O(9)#6	53.6(3)
O(9)#5-Cd(3)-O(9)#6	117.4(4)		

Symmetry transformations used to generate equivalent atoms:

#1 x-y, x-1, -z    #2 -x+y+4/3, y+2/3, z+1/6    #3 -x+4/3, -x+y+2/3, -z+1/6    #4 x-y+1/3, -y+2/3, -z+1/6  
 #5 -y+4/3, -x+2/3, z+1/6    #6 x-y+1, x, -z    #7 y+1, -x+y+1, -z    #8 y, -x+y+1, -z    #9 -x+y+2/3, y-2/3, z-1/6

## S5 References

- [1] H. He, F. Sun, J. Jia, Z. Bian, N. Zhao, X. Qiu, L. Gao and G. Zhu, *Cryst. Growth Des.*, 2014, **14**, 4258.
- [2] G. M. Sheldrick, SADABS, *Program for Empirical Absorption Correction for Area Detector Data*, University of Gottingen, Gottingen, Germany, 1996.
- [3] G. M. Sheldrick, *SHELXTL Version 5.1 Software Reference Manual*, Bruker AXS. Inc., Madison, WI 1997.